Research paper

Temporal variation in soil respiration and its sensitivity to temperature along a hydrological gradient in an alpine wetland of the Tibetan Plateau

Lingfei Yu[a,b], Hao Wang[c], Yonghui Wang[d], Zhenhua Zhang[e], Litong Chen[e], Naishen Liang[f], Jin-Sheng He[a,g,*]

[a] Department of Ecology, College of Urban and Environmental Sciences, Key Laboratory for Earth Surface Processes of the Ministry of Education, Peking University, 5 Yiheyuan Rd., 100871 Beijing, China
[b] State Key Laboratory of Vegetation and Environmental Change, Institute of Botany, Chinese Academy of Sciences, 20 Nanxincun, Xiangshan, 100093 Beijing, China
[c] Institute of Innovation Ecology, Lanzhou University, 768 Jiayuguan W Road, 730020, Lanzhou, China
[d] Department of Ecology, School of Ecology and Environment, Inner Mongolia University, No. 235 West College Road, 010021, Hohhot, China
[e] Key Laboratory of Adaptation and Evolution of Plateau Biota, Northwest Institute of Plateau Biology, Chinese Academy of Sciences, 23 Xining Rd., 810008 Xining, China
[f] Center for Global Environmental Research, National Institute for Environmental Studies, Tsukuba, Ibaraki 305-8506, Japan
[g] State Key Laboratory of Grassland and Agro-ecosystems, College of Pastoral Agriculture Science and Technology, Lanzhou University, 768 Jiayuguan W Road, 730020, Lanzhou, China

ARTICLE INFO

ABSTRACT

Wetlands are predicted to experience lowered water tables due to permafrost degradation in the Tibetan Plateau. These changes may affect carbon cycle processes such as soil respiration (R_s). However, the magnitude, patterns and controls of R_s remain poorly understood in alpine wetlands with their distinct hydrological regimes. Here, we conducted a field study on R_s from 2012 to 2014 in three alpine ecosystems on the Tibetan Plateau—fen, wet meadow and meadow—with soil water decreases along hydrological gradients. From 2012 to 2014, the annual R_s was 128.9–193.3 g C m^{-2}yr^{-1}, 281.5–342.9 g C m^{-2}yr^{-1}, and 663.4–709.1 g C m^{-2}yr^{-1} for the fen, wet meadow, and meadow, respectively. An abrupt increase in CO_2 emissions was caused by the spring thawing of the frozen soil in the fen and wet meadow, contributing 20.4–37.6% and 13.2–17.4%, respectively, to the annual R_s. The diurnal variation in the R_s was site specific among the three ecosystems, with one peak at 1300 h in the fen and meadow and two peaks at 1300 h and 1900 h in the wet meadow. The temperature-independent components of the diurnal variation in R_s were generally explained by photosynthetically active radiation in the fen and wet meadow, but not in the meadow. The temperature sensitivity of the R_s (unconfounded Q_{10}) varied significantly among the three ecosystems, with the highest values occurring in the wet meadow, implying that permafrost thaw-induced wetland drying from the fen to the wet meadow could enhance the response of CO_2 emissions to climate warming but that further drying from the wet meadow to the meadow probably weakens the effect of warming on the R_s. Our study emphasized the important role of the hydrological regime in regulating the temporal variation in R_s and its response to climate warming.

1. Introduction

Wetlands store 20–25% of the total global soil carbon (C) while covering only 4–6% of the land area (Aselmann and Crutzen, 1989; Gorham, 1995; Matthews and Fung, 1987), which plays a critically important role in regulating the atmospheric CO_2 concentrations. Soil respiration (R_s) is the second largest C flux in terrestrial ecosystems, and it exerts a tremendous effect on global C cycling. In a global R_s database, R_s records for wetlands are very limited compared to those available for upland areas despite the large amounts of soil C in wetlands (Bond-Lamberty and Thomson, 2010). Given that climate models predict climate changes throughout this century (IPCC, 2013), the fate of the large store of C in wetlands is of concern, especially in alpine ecosystems, which are vulnerable to climate change (Liu and Chen, 2000).

R_s is strongly linked to several physical (e.g., soil temperature, soil moisture) and biological factors (e.g., photosynthesis) that complicate the mechanistic understanding of R_s (Ryan and Law, 2005). Over a

seasonal scale, R_s variations are commonly expressed as van't Hoff, Arrhenius, or Lloyd and Taylor functions of soil temperature (Davidson et al., 2006). Although soil temperature often accounts for a large fraction of seasonal R_s variation, some of the variability in this apparent response to temperature may result from the confounding effects of other factors, such as the soil moisture or water table in the wetland (Davidson et al., 1998; Miao et al., 2013). Soil water may constrain R_s in two ways, either by limiting aeration and thus the diffusivity of O_2 into the soil, which impedes decomposition and CO_2 production (Linn and Doran, 1984) when soil water is high or by stressing soil microbial activities in the decomposition processes (Schimel et al., 2007) when soil water is very low. Large variations and inconsistences in the responses of R_s to the soil water content have been found in studies on wetland and upland ecosystems (Reichstein et al., 2002; Savage and Davidson, 2001; Silvola et al., 1996). Thus, the response of R_s to soil moisture largely depends on the water availability of the ecosystems (Knapp et al., 2008). On the diurnal scale, many researchers have observed that R_s and soil temperature may be decoupled, showing a diel hysteresis, made evident by semielliptical shapes in plots of soil temperature and R_s (e.g., Gaumont-Guay et al., 2006; Riveros-Iregui et al., 2007). While several studies have postulated that environmental factors that oscillate out of phase with soil temperature, such as photosynthesis, regulate the diurnal R_s variation (Kuzyakov and Gavrichkova, 2010; Liu et al., 2006; Tang et al., 2005), other studies have shown that physical transport processes (heat and CO_2) alone are sufficient to create hysteresis (Phillips et al., 2011). These results largely enhance our knowledge about the temporal variation in R_s driven by abiotic and biotic factors; however, few studies have discussed how R_s varies temporally along hydrological gradients.

The spring thawing of soil is characterized by daily freeze-thaw cycles, which are important short-term transitional and nonstationary phenomena in high-latitude and high-altitude ecosystems that cause abrupt step changes in soil biophysical conditions. The thawing of frozen soils increases the soil water availability and mobilizes nutrients, thereby rapidly shifting plant and microbial activity from dormant states to active states (Henry, 2007; Kim et al., 2012). Thus, an increased CO_2 flux with thawing has been characterized in various uplands and laboratory incubation experiments, as reviewed by Kim et al. (2012) and Matzner and Borken (2008). Alternately, Elberling and Brandt (2003) reported a burst of CO_2 with soil thawing in a tundra heathland, which was attributed to the release of trapped CO_2 from the frozen soil with ice formation. However, some studies have revealed inconsistent results with nonsignificant changes in R_s after thawing (e.g., Groffman et al., 2006; Muhr et al., 2009). Since soil moisture influences thawing and freezing processes, we hypothesized that soil water conditions may regulate the responses of soil CO_2 flux to thawing and freezing. Additionally, discrete measurements, e.g., measuring weekly or monthly during the thawing and freezing period, would have missed the peak fluxes of R_s due to their short response period (Kim et al., 2012). Thus, to improve our understanding of the biophysical effects of soil thawing and freezing on R_s, R_s measurements with high temporal resolution, e.g., hourly, are needed from alpine ecosystems with different hydrological conditions.

The Tibetan Plateau, the largest geomorphological unit on the Eurasian continent, is an important part of the global terrestrial ecosystem, with a mean elevation of ~4000 m. The plateau has the largest extent of permafrost in the high-altitude region, with the permafrost area of approximately 1.35×10^6 km^2, covering ~67% of the plateau area (Ran et al., 2012). Alpine wetland ecosystems occupy an area of 0.049×10^6 km^2 on the Tibetan Plateau, accounting for 2.5% of the plateau area (Sun and Zheng, 1996). These ecosystems are typically underlain by permafrost and maintain a water table near the surface (Baumann et al., 2009). However, given that the annual mean surface air temperature would rise by 1.4–2.2 °C in the next 30–50 years on the plateau (Liu et al., 2009), the wetlands are predicted to have lowered water tables due to the permafrost degradation caused by rapid climate

warming (Cheng and Wu, 2007). It was estimated that over 10% of the alpine wetland in the plateau was degraded from 1967 to 2004 (Zhang et al., 2011). Permafrost degradation could expose significant quantities of organic carbon to decomposition by soil microbes, and then permafrost thaw-induced soil drying would accelerate organic matter decomposition (Lawrence et al., 2015; Schuur et al., 2015). Thus, a better understanding of CO_2 emissions from wetlands to upland slopes is needed to evaluate the effect of hydrological changes on R_s on the plateau.

We conducted a 3-year field experiment of R_s along a hydrological gradient in the alpine wetland of the Tibetan Plateau. Three types of vegetation were defined—fen, wet meadow and meadow—with soil water decreasing along the hydrological gradient. Automated chambers were set up to record the hourly measurements of R_s. The main objectives were (1) to quantify the total annual R_s of the three ecosystems, (2) to investigate the seasonal and diurnal variations in R_s and their environmental drivers along the hydrological gradients, and (3) to examine the biophysical effects of the freeze-thaw process on R_s under different hydrological conditions. We hypothesized that (1) annual R_s changes among the three ecosystems largely due to different water tables or water availability; (2) R_s is affected by abiotic factors, e.g., soil temperature, soil moisture/water table and photosynthetic active radiation (PAR), but the correlation between R_s and the factors may change along the hydrological gradients because soil water conditions could regulate the oxygen and substrate availability and hence affect the microbial activity; and (3) thawing of frozen soil causes pulses of R_s due to the sudden flushes of soil water and nutrient availability or release of the trapped CO_2 in the frozen soil.

2. Materials and methods

2.1. Site description

This study was conducted at the Luanhaizi alpine wetland, adjacent to the Haibei Alpine Grassland Ecosystem Research Station (37°30′N, 101°12′E, 3200 m a.s.l.) in the northeastern part of the Tibetan Plateau, China (Fig. 1a). This area is underlain by permafrost, which is in a state of degradation (Wang et al., 2015). The area has a continental monsoon climate with short summers and long winters. From 1981 to 2010, the mean annual air temperatures were −1.1 °C, and the mean annual precipitation was 480 mm, of which more than 80% was concentrated from May to September. There was no thick (<10 cm) and persistent snowpack in the nongrowing season, and the number of days of snow was only 20–34 days (Wang et al., 2014). The air pressure was low, approximately 70 kPa, due to the high altitude.

Three types of ecosystems are distributed along the topographic gradient in the study area: fen, wet meadow, and meadow (Fig. 1b and c). The fen is a flat field, located at the lowest elevations and characterized by a unique microtopography with many scattered hummocks (Fig. 1d). The community is dominated by *Carex pamirensis* C. B. Clarke ex B. Fedtsch. rooted in shallow peat, along with several other species, including *Carex atrofusca* Schkuhr, *Hippuris vulgaris* L., *Triglochin palustre* L., and *Heleocharis* spp. The fen is generally constantly flooded from June to late October and is covered by ice from early November to the following early April. The wet meadow is a gentle slope (< 10°) located at the middle elevation and is distributed along the margin area of the fen (Fig. 1e). The community is dominated by *Kobresia tibetica* Maxim., *Blysmus sinocompressus* Tang et Wang, and *C. atrofusca* Schkuhr, and a continuous layer of moss species forms the ground layer. The wet meadow surface is never flooded, but the soil remains nearly saturated throughout the year. The meadow, adjacent to the wet meadow and approximately 100 m apart from the fen, is located at the highest elevation (Fig. 1f). Its community is dominated by *Stipa aliena* Keng, *Elymus nutans* Griseb., and *Helictotrichon tibeticum* (Roshev.) Holub. The meadow never experiences flooding, and its soils are drier than those of the wet meadow. The characteristics of the climate, soil
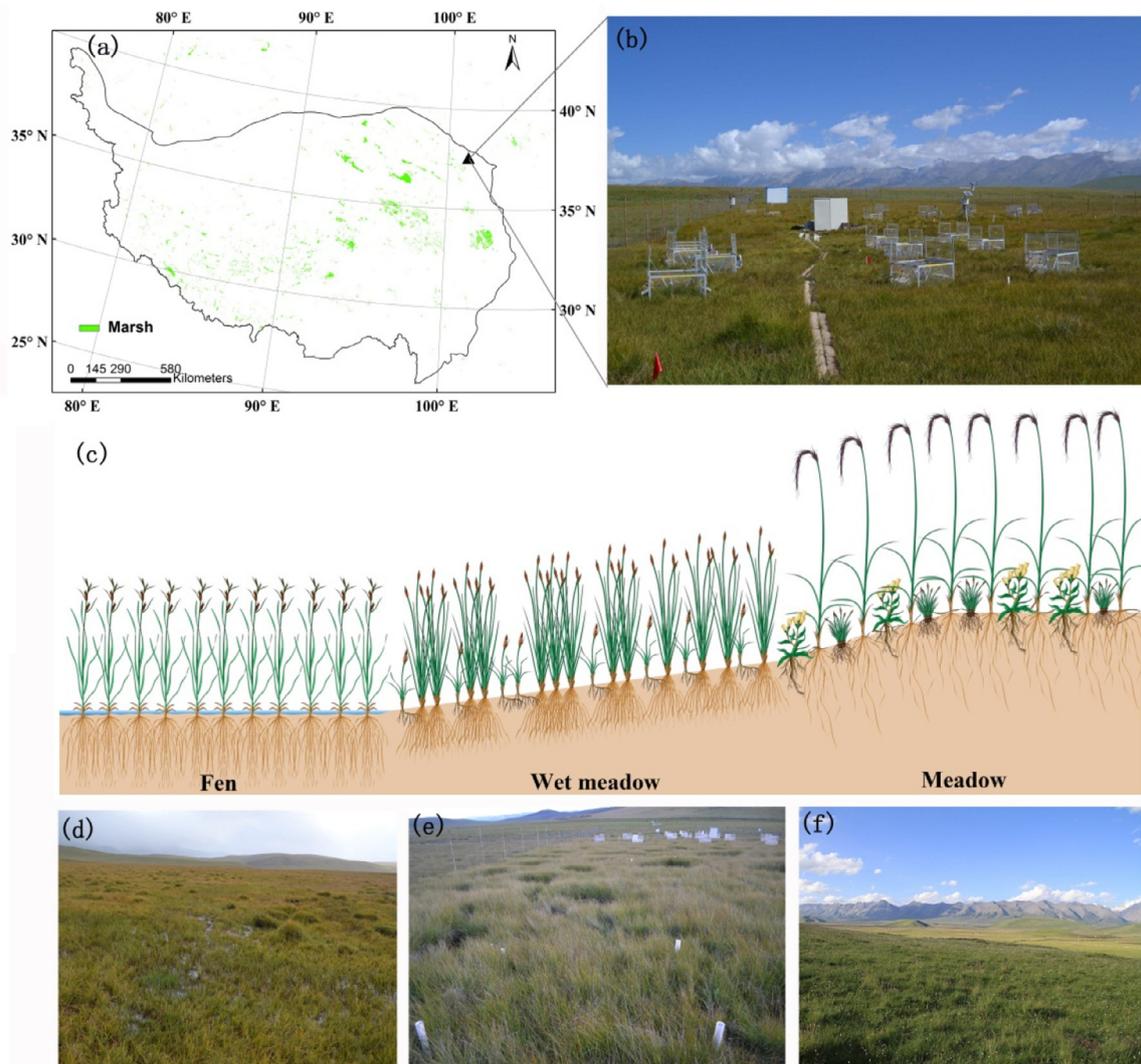
Fig. 1. The study site along the hydrological gradient in the alpine wetland of the Tibetan Plateau: (a) geographic location with the wetland distribution map sourced from Niu et al. (2012); (b) landscape; (c) sketch map of the site; (d) fen; (e) wet meadow; and (f) meadow (1.5 column).

and vegetation are detailed in Table 1.

2.2. R_s measurements

From early August 2011 to late October 2014, R_s was measured in a flow-through and nonsteady-state manner using a custom-designed, multichannel, automated, chamber system in the fen and wet meadow. This system comprised a control unit inside a field-accessible case and 20 automated chambers. The main component of the control unit was a datalogger (CR1000, Campbell Scientific Inc., Logan, UT, USA), a two-valve manifold (CKD-LAC-V-4SB010, CKD Corp., Nagoya, Japan), a micro infrared gas analyzer (IRGA; Li-Cor 840, Li-Cor, Lincoln, NE, USA), a $CO_2/CH_4/H_2O$ gas analyzer (Picarro G1301, Picarro, Santa Clara, CA, USA), and a 62-differential-channel sensor multiplexer. The chambers (90 cm long × 90 cm wide × 50 cm tall) were made of clear PVC glued to an aluminum frame. Between measurements, the chamber lid is open and allows precipitation to reach the enclosed soil surface, thus keeping the soil conditions as natural as possible. During the measurements, the chamber lid is closed, and the chamber air is sampled continuously from the chamber to the IRGA and $CO_2/CH_4/H_2O$ gas analyzer for concentration measurement. The gas fluxes are calculated from the change in the gas concentration over time within the chamber. The chambers were programmed by the CR1000 datalogger to close and open sequentially for measuring within the hour-long cycle. The

measuring period for each chamber was set to 3 min to finish a cycle of measurements within 1 h. This system has been previously described in detail (Liang et al., 2017; Yu et al., 2013). In this study, we only used R_s (soil CO_2 flux) measurement data from 10 of the 20 chambers, with 5 chambers in the fen and 5 in the wet meadow. The other 10 chambers were used to measure the net ecosystem CO_2 exchange. The chambers were randomly distributed at each site and maintained at the same location throughout the study period.

The continuous R_s measurement in the meadow was conducted at another study site, which is approximately 1.5 km away from the fen and wet meadow. The soil hydrology and vegetation in the meadow are similar to those adjacent to the wet meadow. The R_s in this site was measured with a Li-8150 multiplexer automated soil CO_2 flux system (Li-Cor Inc., Lincoln, NE, USA). The R_s measurements were taken on PVC collars (20 cm in diameter and 10 cm in height) that were inserted 4 cm into the soil. Three spatial chamber replicates were established at the site. Each chamber was sealed on the collar during the measurements, and the instrument recorded the CO_2 concentration. The R_s was calculated using a linear or exponential regression model with Li-8100 file viewer application software (LI-8100/8150, Instruction Manual). The R_s within each chamber was measured at intervals of 1 h. The measuring period for the R_s of each chamber was 5 min. During the other period, the chamber was opened for aeration.

Table 1

Climate, soil and vegetation characteristics in the three ecosystems on the Tibetan Plateau[a].

	2012	2013	2014
Mean annual air temperature (˚C)	−1.82	−1.08	−1.36
Annual precipitation (mm)	367	403	573
Photosynthetically active radiation ($\mu mol\ m^{-2}s^{-1}$)	357	383	397
Fen			
Mean annual soil temperature at 5 cm (˚C)	2.37 ± 0.26	2.58 ± 0.28	1.69 ± 0.38
Mean annual soil temperature at 30 cm (˚C)	1.25	1.33	1.59
Mean water table (cm)[b]	−0.96	−0.12	0.55
Soil pH	7.7 ± 0.4		
Soil total carbon (%)	16.0 ± 3.8	—	—
Soil total nitrogen (%)	1.1 ± 0.22	—	—
Aboveground biomass ($g\ m^{-2}$)	224.1 ± 42.3	206.9 ± 58.1	289.0 ± 49.0
Belowground biomass ($g\ m^{-2}$)	—	—	6592 ± 1878
Wet meadow			
Mean annual soil temperature at 5 cm (˚C)	2.48 ± 0.18	3.08 ± 0.20	2.52 ± 0.24
Mean annual soil temperature at 30 cm (˚C)	2.46	2.28	2.44
Mean annual soil moisture at 10 cm (v/v,%)[c]	45.4	50.8	60.2
Soil pH	7.6 ± 0.4		
Soil total carbon (%)	23.0 ± 2.91	—	—
Soil total nitrogen (%)	1.7 ± 0.45	—	—
Aboveground biomass ($g\ m^{-2}$)	323.3 ± 56.1	258.0 ± 66.0	345.3 ± 39.8
Belowground biomass ($g\ m^{-2}$)	—	—	7514 ± 1641
Meadow			
Mean annual soil temperature at 5 cm (˚C)	4.51	5.02	5.26
Mean annual soil temperature at 30 cm (˚C)	2.81	2.85	2.93
Mean annual soil moisture at 10 cm (%)[d]	21.5	22.6	29.7
Soil pH	8.3 ± 0.1		
Soil total carbon (%)	5.7 ± 0.67	—	—
Soil total nitrogen (%)	0.5 ± 0.067	—	—
Aboveground biomass ($g\ m^{-2}$)	387.1 ± 18.8	291.7 ± 52.1	355.7 ± 68.2
Belowground biomass ($g\ m^{-2}$)	—	—	1745 ± 364

[a] Some values represent the mean ± standard deviation ($n = 5$).

[b] The water table was measured from April 25 to October 16 in 2012, from April 25 to October 29 in 2013, and from April 25 to October 25 in 2014.

[c], [d] Soil moistures in the wet meadow and meadow were measured during the thawed season.

Table 2

The cumulative soil respiration (R_s) of the different seasons and their contributions to the annual total R_s for the three ecosystems.

	2012 R_s ($g\ C\ m^{-2}$)	Contribution (%)	2013 R_s ($g\ C\ m^{-2}$)	Contribution (%)	2014 R_s ($g\ C\ m^{-2}$)	Contribution (%)
Fen						
thawing	72.8 ± 8.4c	37.6 ± 2.2c	38.9 ± 4.4b	24.9 ± 1.9c	26.3 ± 3.3a	20.4 ± 1.3c
thawed	106.0 ± 11.4a	54.8 ± 1.7a	103.1 ± 17.3a	65.5 ± 2.8a	85.4 ± 11.4a	66.2 ± 1.7a
freezing	2.2 ± 0.086a	1.1 ± 0.11a	1.9 ± 0.17a	1.2 ± 0.13b	3.2 ± 0.54a	2.5 ± 0.24b
frozen	12.4 ± 1.5a	6.5 ± 1.0b	13.0 ± 0.65a	8.4 ± 1.4c	13.9 ± 1.2a	10.9 ± 1.8c
total	193.3 ± 18.0a	—	156.9 ± 20.6a	—	128.9 ± 14.2a	—
Wet meadow						
thawing	53.0 ± 3.7b	15.5 ± 1.2b	52.8 ± 5.2c	17.4 ± 1.6b	37.0 ± 3.2b	13.2 ± 1.2b
thawed	259.0 ± 22.1b	75.5 ± 1.6b	230.5 ± 19.8b	75.9 ± 1.7b	215.7 ± 18.4b	76.6 ± 1.9b
freezing	5.8 ± 0.32b	1.7 ± 0.17b	4.8 ± 0.14b	1.6 ± 0.082c	10.8 ± 0.63c	3.8 ± 0.40c
frozen	23.8 ± 0.63c	7.0 ± 0.60b	15.3 ± 0.65b	5.1 ± 0.36b	18.1 ± 0.69b	6.4 ± 0.36b
total	342.9 ± 23.1b	—	303.4 ± 22.2b	—	281.5 ± 19.2b	—
Meadow						
thawing	32.9 ± 2.7a	4.6 ± 0.40a	24.4 ± 1.6a	3.7 ± 0.33a	25.0 ± 1.9a	3.7 ± 0.22a
thawed	645.5 ± 23.6c	91.0 ± 0.87c	615.3 ± 21.6c	92.7 ± 0.63c	616.3 ± 82.2c	91.7 ± 1.2c
freezing	10.5 ± 1.3c	1.5 ± 0.21b	5.7 ± 0.24c	0.86 ± 0.057a	8.3 ± 1.1b	1.2 ± 0.26a
frozen	20.3 ± 1.7b	2.9 ± 0.30a	17.9 ± 1.3c	2.7 ± 0.26a	21.7 ± 2.2c	3.3 ± 0.71a
total	709.1 ± 21.1c	—	663.4 ± 19.1c	—	671.2 ± 82.2c	—

Values represent the mean ± standard deviation ($n = 5$ for the fen and wet meadow, and $n = 3$ for the meadow). Letters within a column indicate a significant difference in cumulative R_s or their contributions to annual R_s among the ecosystems in the same season ($P < 0.05$).

2.3. Environmental measurements

Half-hourly data on air temperature, precipitation and photosynthetic active radiation (PAR) were collected from a meteorological station located in the wet meadow. The topsoil temperature was continuously measured every 30 min at a depth of 5 cm in the fen with a type T thermocouple connected to a CR1000 datalogger when the multichannel automated chamber system was being operated. The soil temperature was automatically measured hourly at depths of 10 cm and 30 cm by EM50 sensors (Decagon Devices Inc., USA). The water table height in the fen was automatically recorded hourly by HOBO dataloggers (Onset Computer, Bourne, MA, USA). In the wet meadow, the topsoil temperatures (5 cm, 10 cm and 30 cm) were continuously measured every 30 min with a type T thermocouple connected to the CR1000 datalogger. The topsoil moisture (10 cm;% v/v) was collected every half-hour from a meteorological station located at this site. In the meadow, the topsoil temperature (5 cm and 10 cm) and moisture (10 cm;% v/v) were automatically measured hourly by EM50 sensors
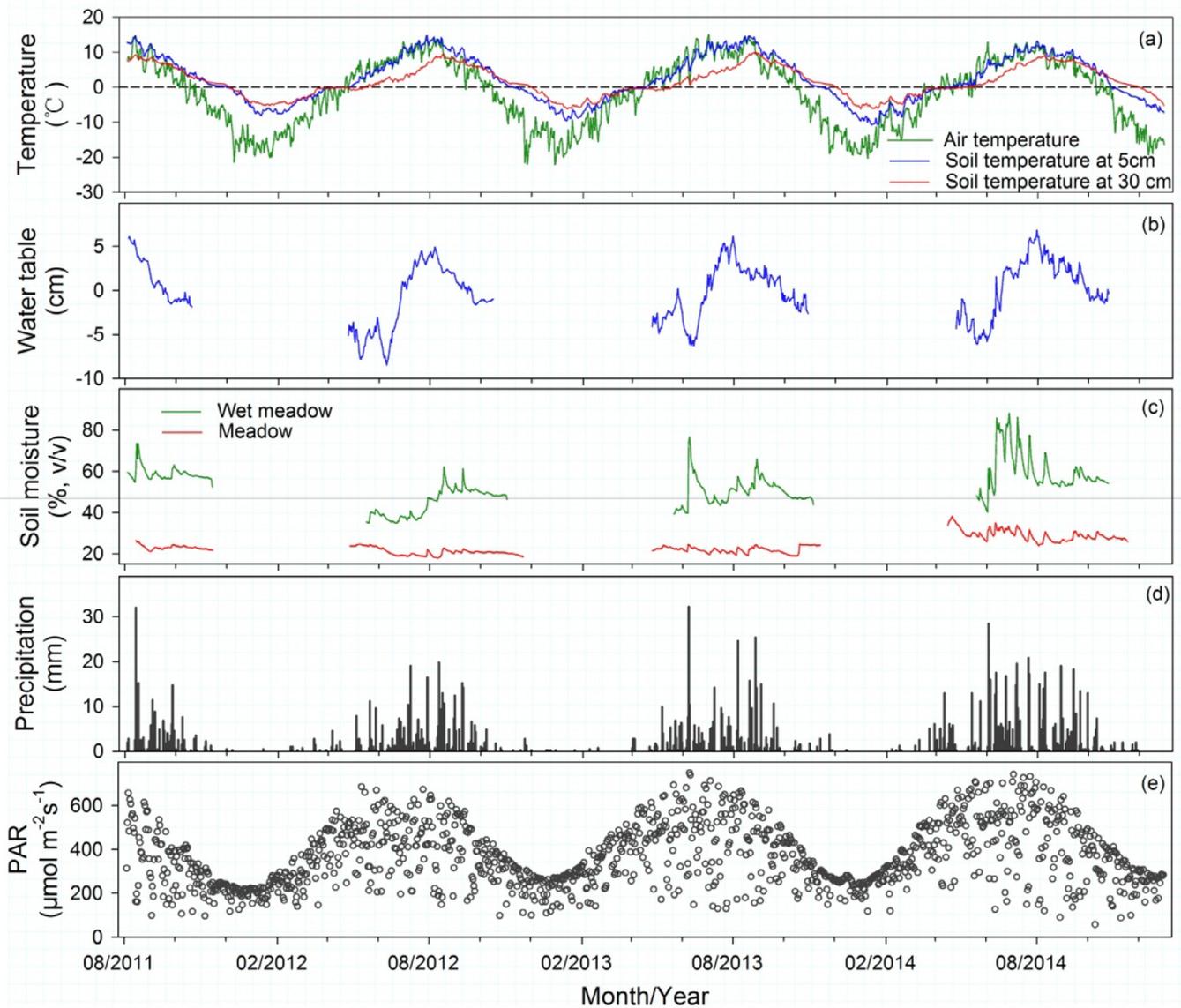
Fig. 2. Environmental factors of the study site from 2011 to 2014: (a) daily average air temperature and soil temperature in the fen; (b) water table in the fen; (c) soil moisture in the wet meadow and meadow when the soil was thawed; (d) daily cumulative precipitation; and (e) daily average photosynthetically active radiation (PAR). Since soil temperatures showed similar seasonal patterns among the three ecosystems, the seasonal variations for the wet meadow and meadow were not shown. The dotted line indicates the temperature at zero (2 column).

(Decagon Devices Inc., USA). Soil temperature at 30 cm depth was provided by another meteorological station located in the meadow.

2.4. Specified season definition

The year was divided into four time periods based on the soil temperature at depths of 5 cm and 30 cm: thawing, thawed, freezing and frozen soil (Supplementary Table S1). Thawing soil was defined as the period that starts from the first of three consecutive days when the daily maximum soil temperature at 5 cm depth was above 0 °C to the first of three consecutive days when the daily minimum soil temperature at 30 cm was above 0 °C. Freezing soil was defined as the period ranging from the first of three consecutive days when the daily minimum soil temperature at 5 cm depth was below 0 °C to the first of three consecutive days when the daily maximum soil temperature at 30 cm depth was below 0 °C. Thawed soil ranges from the end of thawing to the start of freezing. Frozen soil ranges from the end of freezing to the start of thawing in the next year. The soil surface temperature (0 cm) was expected to more accurately define the start time of

the thawing and freezing soil. Unfortunately, the surface temperature was not measured in the fen and wet meadow; thus, we used the temperature at 5 cm instead of the surface temperature. A soil temperature at 30 cm was used to define the end of the thawing and freezing periods because more than 90% and 80% of the belowground biomass was distributed in the top 30 cm of the soil in the alpine meadow and wetland, respectively (Ma et al., 2017; Yang et al., 2009).

2.5. Data analysis

We used an exponential function to examine the relation between R_s and temperature as follows:

$$R_s = \exp^\alpha \times \exp^{\beta \times T} \tag{1}$$

where R_s is the soil respiration rate, T is the air or soil temperature, $\exp^\alpha$ is the fitted R_s at 0 °C air or soil temperature, and β is the sensitivity of the R_s to temperature. A natural logarithm transformation of R_s was conducted, and the above equation then yielded the following:
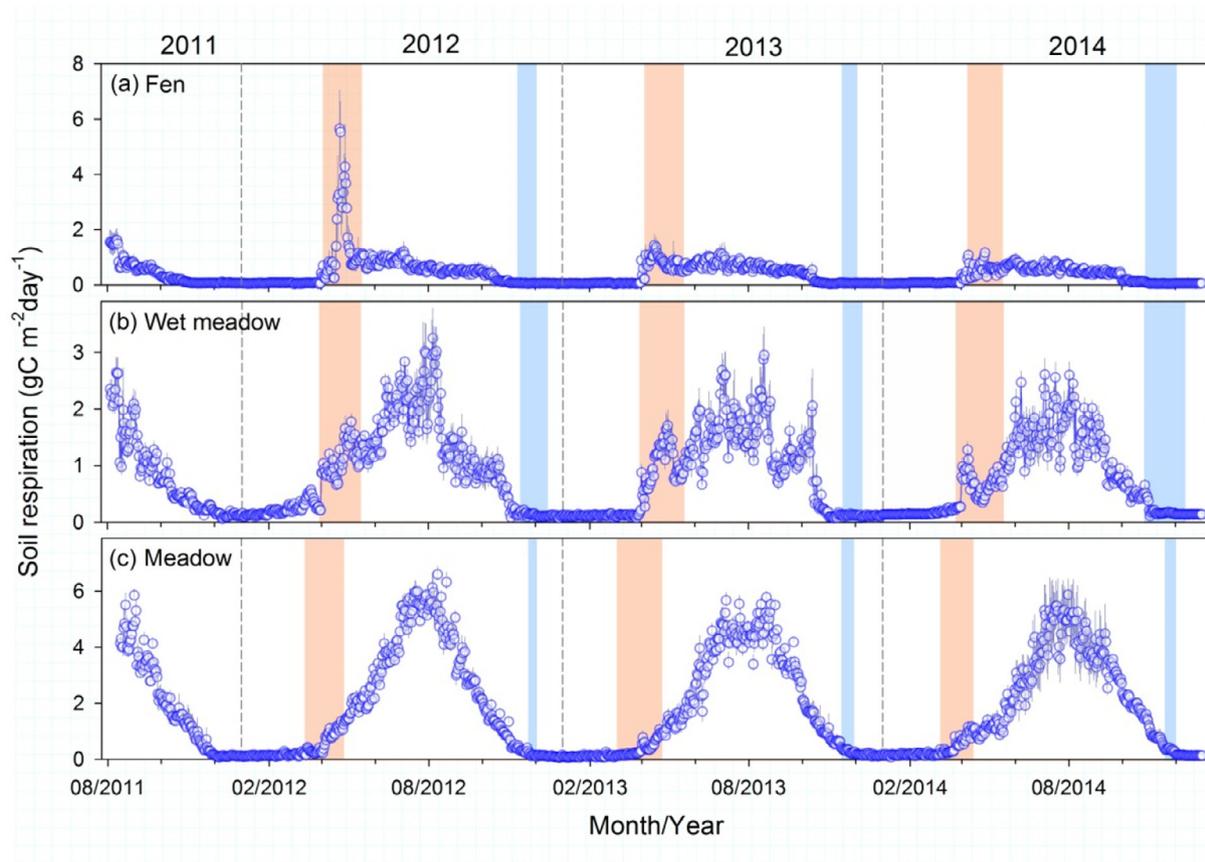
Fig. 3. Seasonal variations in daily soil respiration in the fen (a), wet meadow (b) and meadow (c) from 2011 to 2014. The periods of spring thawing and autumn freezing are shaded in light red and blue, respectively. Error bars represent the standard deviation of the means ($n = 5$ for the fen and wet meadow, and $n = 3$ for the meadow) (2 column).

$$\mathrm{Ln}R_s = \alpha + \beta \times T \qquad (2)$$

The Q_{10} value, which represents the temperature response of the R_s, was calculated as follows:

$$Q_{10} = \exp^{10 \times \beta} \qquad (3)$$

Nonetheless, this estimated Q_{10} may contain the influences of nontemperature-driven confounding factors that seasonally covary with temperature, e.g., vegetation activity (Wang et al., 2010; Yuste et al., 2004), and thus does not accurately represent the responses of the R_s to the temperature change (Wang et al., 2018). To minimize the influence of confounding effects, we applied singular spectrum analysis (SSA), a highly data-adaptive method for subsignal separation, to estimate the Q_{10} of the R_s. The time series of both the temperature and the log-transformed R_s were first partitioned into subsignals with different frequencies. According to Mahecha et al. (2010), a period of 100 days was chosen as the threshold that divides the high-frequency bins from the low-frequency bins. We can then estimate the temperature sensitivities derived from the specific subsignals (high-frequency) with eqn. (3) such that confounding factors generally corresponding to the low-frequency subsignals are excluded. Our key assumption is that low-frequency signals are assumed to contain the nontemperature-driven confounding effects (Gu et al., 2008; Mahecha et al., 2010).

We also used simple linear regression analysis to investigate the relationship among R_s and other abiotic factors, e.g., the soil moisture, water table and PAR. Empirical models relating seasonal variation in R_s to air or soil temperature, soil moisture or water table and PAR were developed for each vegetation type using multiple linear regressions. To avoid multiple collinearity, the variables with VIF (variance inflation factor) < 4 were selected for the multiple linear regressions. We then used standardized regression coefficients to compare the relative

importance of the predictive variables. A natural logarithm transformation of R_s was used to achieve linearity and homoscedasticity in the regression analysis. We only investigated the effect of abiotic factors on R_s during the thawed season because the soil during the other seasons (freezing, frozen and thawing) was generally frozen or subject to freeze-thaw cycles, which primarily controlled the CO_2 emissions (Wang et al., 2014).

Data filtering, as well as instrument malfunction, created large gaps in the data series, with 20–32% of gaps (hours to days) from April to October and 46–79% of gaps (up to months) from November to March (Supplementary Fig. S1); hence, all of the data gaps were filled to estimate the daily, seasonal and annual values of the R_s. A back-propagation artificial neural network was employed to gap-fill the missing hourly R_s data. In keeping with the principle of parsimony and good gap-filling performance, the following variables usually measured at the field sites were included: air temperature, soil temperature, water table (fen) or soil moisture (wet meadow and meadow), relative humidity, and PAR, together with the fuzzy sets representing the seasonal variation and time of day (Papale and Valentini, 2003). We included the same input variables and five neurons for all datasets from the three ecosystems. Data obtained from each chamber were proportionally sampled into a training (70%) and a test (30%) dataset for artificial neural network analysis, which covered all meteorological and flux variability. Each analysis ran 500 times, of which the 25 best runs were selected in the gap filling according to the lowest values of the root mean square error. The hourly values of R_s were summed to calculate the cumulative daily, seasonal and annual values of R_s. The data gap in the soil temperature in the fen and wet meadow was filled with the data from the nearby EM50 (Decagon Devices Inc., USA) and the meteorological station, respectively. The significance of the differences in the
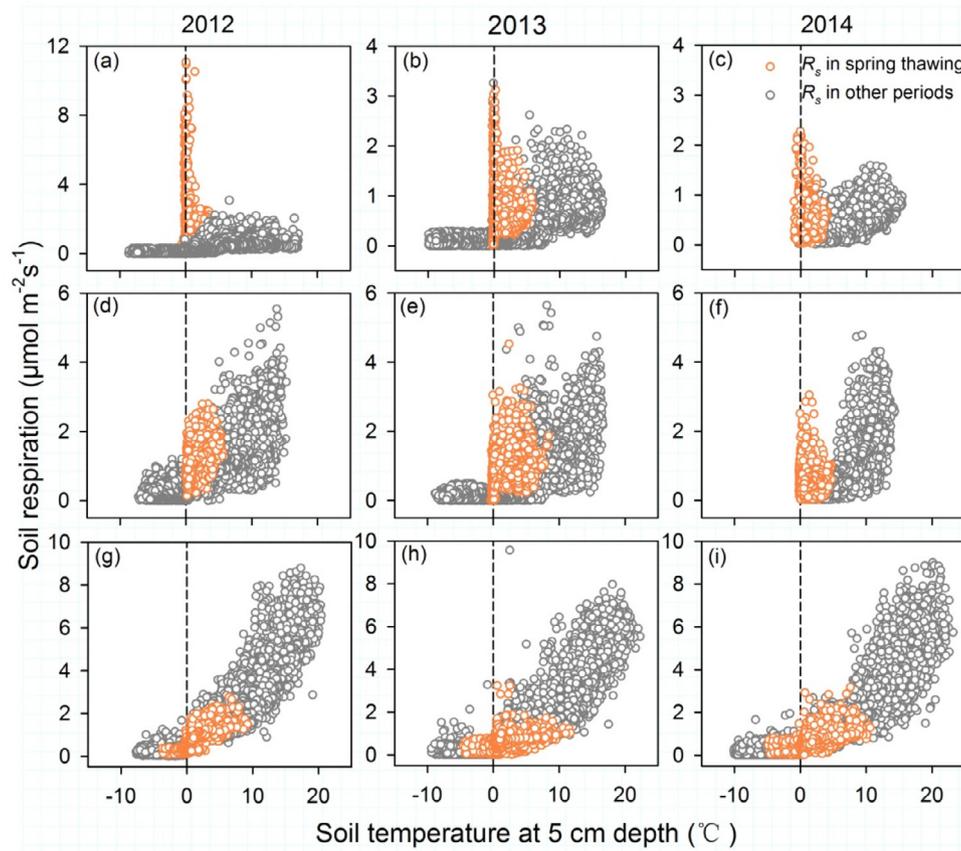
Fig. 4. The change in hourly soil respiration (R_s) with soil temperature at 5-cm depth in the fen (a-c), wet meadow (d-f), and meadow (g-i) in 2012, 2013 and 2014. The hourly respiration data were not gap-filled. The dotted lines indicate the soil temperature at zero (1.5 column).

cumulative R_s and Q_{10} among the three ecosystems was analyzed using a one-way analysis of variance (ANOVA). All statistical analyses were performed using R version 3.3.1 (The R Foundation for Statistical Computing, Vienna, Austria, 2016), with the package *Rssa* for SSA and the package *AMORE* for the artificial neural network analysis.

3. Results

3.1. Overall estimates

During the observation period of 2012–2014, the annual R_s for the fen, wet meadow and meadow varied significantly ($P < 0.001$) and averaged 159.7 ± 32.3, 309.3 ± 31.1 and 681.2 ± 24.4 (mean ± SD) g C m^{-2}yr^{-1} across the three years, respectively, for the three ecosystems (Table 2). The seasonal R_s values and their contributions to annual emissions also varied greatly among the three ecosystems ($P < 0.05$; Table 2). The R_s during the thawing season accounted for 20.4–37.6% of the total annual R_s in the fen, which is higher than that observed in the wet meadow (13.2–17.4%) and the meadow (3.7–4.6%). In contrast, the thawed season R_s accounted for more than 90% of the total annual R_s in the meadow, followed by the wet meadow (75.5–76.6%) and the fen (54.8–66.2%).

Large variations in R_s among the years were also observed in the three ecosystems, especially in the fen and wet meadow (Table 2). The annual R_s decreased from 2012 to 2014 and was negatively related to the pattern of the water table in the fen and the soil moisture in the wet meadow (Table 1), indicating that soil water may regulate the inter-annual variation in the R_s.

3.2. Seasonal pattern of environmental factors and R_s

Obvious seasonal variations in environmental factors were observed from August 2011 to December 2014 (Fig. 2). Daily average air and soil temperature exhibited apparent cosine-like seasonal patterns (Fig. 2a). The air temperature increased from January to August and then declined gradually, ranging from -22.0 to 15.1 °C. Soil temperatures showed similar seasonal patterns among the three ecosystems; that is, the soil temperatures in the three ecosystems showed the maximum temperature appearing around early August at a depth of 5 cm and around the middle of August at a depth of 30 cm from 2012 to 2014. The water table in the fen was lowest in early June; then, it approached the soil surface in late June and remained above the surface (Fig. 2b). During the thawed season, the soil moisture varied largely with rainfall events, especially in the wet meadow (Fig. 2c and d). The total annual precipitation was generally concentrated in the period from May to September (Fig. 2d). Photosynthetic active radiation (PAR) exhibited a pronounced seasonal pattern, with the daily maximum occurring in late June (Fig. 2e).

In the fen, a clear CO_2 burst occurred during the thawing season, especially in 2012; the emission rates could be as high as 5.67 g C m^{-2}day^{-1} in 2012, 1.46 g C m^{-2}day^{-1} in 2013 and 1.20 g C g C m^{-2}day^{-1} in 2014, which are higher in magnitude than those in the thawed season (Fig. 3a; Supplementary Table S2). The observed CO_2 burst lasted from early April to late April or early May, and after that, the emission rate decreased to the normal rate for the thawed season. In the wet meadow (Fig. 3b) and meadow (Fig. 3c), the R_s showed little variation during the frozen season and then increased gradually as the soil was thawing. A spike in R_s occurred during the thawing period of each year in the wet meadow, but no spikes were found in the meadow. The peak time of seasonal R_s in the wet meadow and meadow occurred
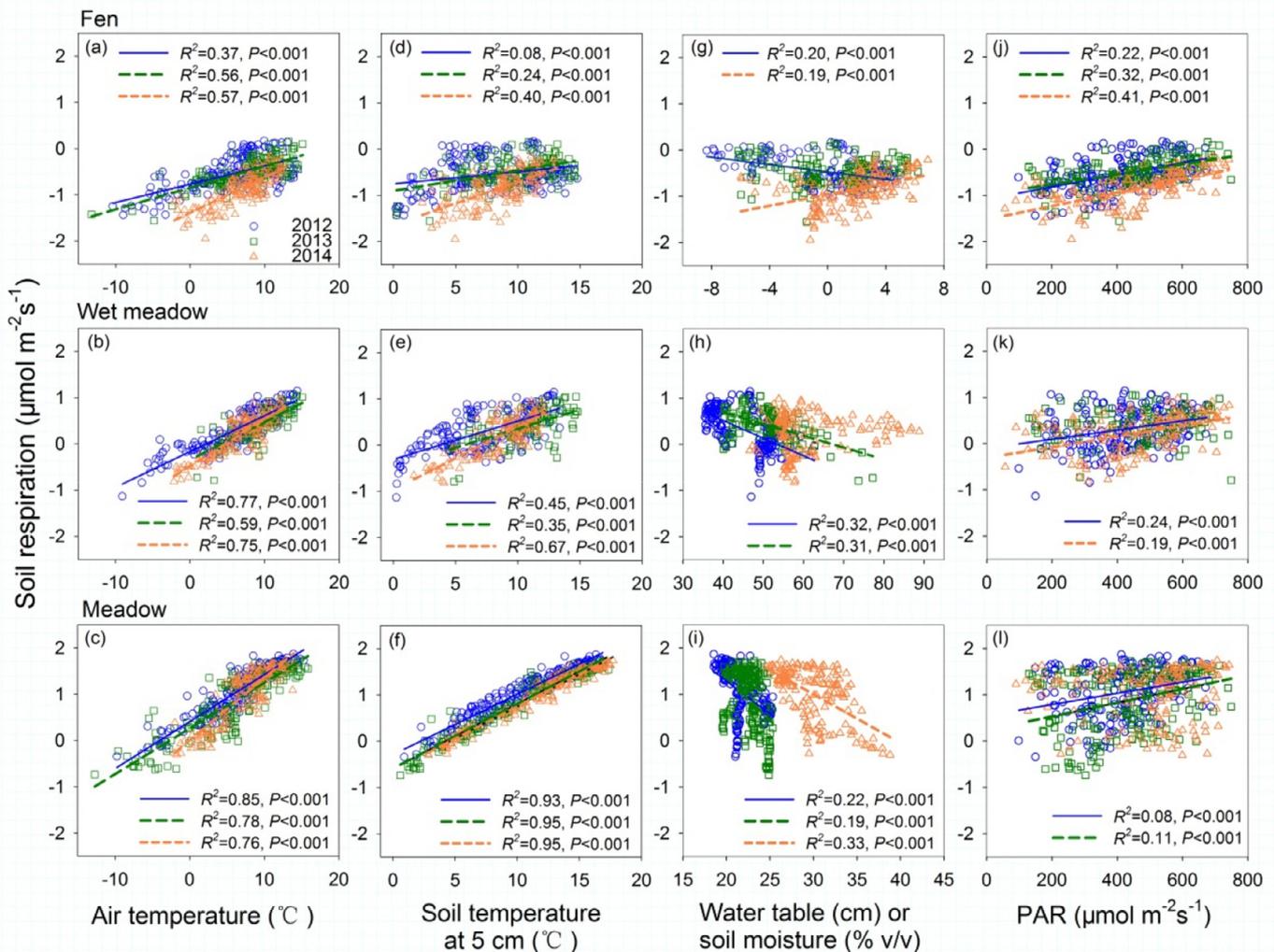
Fig. 5. The relation between the daily average soil respiration and the air temperature (a–c), the soil temperature at 5-cm depth (d–f), the water table or soil moisture at 10-cm depth (g–i), and the photosynthetically active radiation (PAR; j-l) in the fen (a, d, g and j), wet meadow (b, e, h and k) and meadow (c, f, i and l) during the thawed seasons of 2012, 2013 and 2014. The dots represent daily average soil respiration. The solid, medium and short dashed lines are regressions for the data of 2012, 2013 and 2014, respectively. Logarithmic scales were used for the dependent variables of soil respiration (2 column).

around early August, generally coinciding with the time of the peak value of soil temperature at a depth of 5 cm.

3.3. Abiotic controls on R_s

The observed CO_2 burst matched the time period of soil thawing in the fen (Fig. 3a) and wet meadow (Fig. 3b), indicating that the CO_2 burst may be associated with the soil thawing along the soil profile. To confirm the effects of soil thawing on the CO_2 burst, we further analyzed the relationship between hourly R_s and soil temperatures. An abrupt increase in CO_2 emission with the soil temperature occurred when the temperature at a depth of 5 cm was poised at zero from 2012 to 2014 in the fen (Fig. 4a-c) and the wet meadow (Fig. 4d-f). Therefore, the observed CO_2 bursts resulted from the spring thaw of the frozen soil, whereas no obvious abrupt increase in CO_2 emission was observed with increasing soil temperature in the meadow (Fig. 4g-i).

We explored the effect of temperature, water table or soil moisture and PAR on the temporal variation in R_s when the soil was completely thawed. In 2012, 2013 and 2014, the R_s were strongly positively correlated with the air (Fig. 5a-c) or soil temperature at a depth of 5 cm (Fig. 5d-f) based on the daily average data in the three ecosystems. Air temperature could explain more of the variations in the R_s than soil

temperature in the fen (Fig. 5a and d; $R^2 = 0.37$–0.57 *vs.* $R^2 = 0.08$–0.40) and wet meadow (Fig. 5b and e; $R^2 = 0.59$–0.77 *vs.* $R^2 = 0.35$–0.67); however, soil temperature could explain the more than 90% variation in the R_s in the meadow (Fig. 5c and f). The R_s decreased with the water table in 2012 but had no relation with it in 2013 in the fen (Fig. 5g). Surprisingly, the R_s tended to increase with the water table in 2014. The R_s in the wet meadow was negatively correlated with soil moisture in 2012 and 2013 (Fig. 5h). Changes in the soil moisture could explain 31–32% of the variation in the R_s for the two years. Soil moisture also negatively affected the R_s over the three years in the meadow, accounting for 19–33% of the variation in the R_s (Fig. 5i). In contrast, the R_s was generally positively correlated with PAR in the three ecosystems (Fig. 5j-l).

The results of the multiple linear regressions showed that 65–76% in the fen, 75–84% in the wet meadow and 95% in the meadow of the temporal variation in R_s could be accounted for by a model including temperature, water table or soil moisture and PAR (Table 3, Supplementary Table S3). Temperature is the dominant factor in controlling R_s during the thawed season. When the temperature and PAR were controlled, the R_s was generally negatively regressed to the water table and soil moisture in the fen and wet meadow, respectively. In the meadow, however, the soil moisture had a positive effect, little effect, and a

Table 3

Parameters of the regressions between the daily average soil respiration rate (μmol m^{-2}s^{-1}) and air (AT, °C) or soil temperature at a 5-cm depth (ST5, °C), water table (WT, cm) or soil moisture (SM,% v/v) and photosynthetic active radiation (PAR, μmol m^{-2}s^{-1}) during the thawed-soil seasons of 2012, 2013 and 2014 in the three ecosystems. Only one variable of the temperatures (air or soil temperature) with larger explanatory power was selected in the multiple regressions, as shown in Fig. 4. The soil respiration data were log-transformed in the regression analysis. β, regression coefficients; SE, standard error of regression coefficients; $β_{Standardized}$, standardized regression coefficients; VIF, variance inflation factor.

	2012 β	SE	t-value	P	$β_{Standardized}$	VIF	2013 β	SE	t-value	P	$β_{Standardized}$	VIF	2014 β	SE	t-value	P	$β_{Standardized}$	VIF
Fen																		
AT	0.051	0.0044	11.75	<0.001	0.8	1.31	0.042	0.0036	11.81	<0.001	0.86	1.16	0.063	0.0045	14.11	<0.001	0.63	1.11
WT	−0.066	0.0048	−13.78	<0.001	−0.63	1.27	−0.014	0.0048	−2.87	0.0048	−0.13	1.1	—	—	—	—	—	—
PAR	0.0007	0.00012	6.06	<0.001	0.25	1.03	0.0007	0.000095	7.39	<0.001	0.35	1.07	0.001	0.0001	10.15	<0.001	0.44	1.11
Wet meadow																		
AT	0.068	0.0029	23.49	<0.001	0.77	1.14	0.073	0.0051	14.31	<0.001	1.16	1.05	0.095	0.0049	19.54	<0.001	0.81	1.11
SM	−0.02	0.0022	−9.08	<0.001	−0.3	1.14	−0.019	0.0022	−8.49	<0.001	−0.35	1.05	—	—	—	—	—	—
PAR	—	—	—	—	—	—	—	—	—	—	—	—	0.00048	0.00011	4.4	<0.001	0.18	1.11
Meadow																		
ST5	0.14	0.003	46.09	<0.001	1.04	1.74	0.14	0.0023	60.46	<0.001	0.96	—	0.14	0.003	45.82	<0.001	1.07	1.46
SM	0.035	0.0067	5.26	<0.001	0.11	1.7	—	—	—	—	—	—	−0.0082	0.0038	−2.18	0.031	−0.04	1.46
PAR	0.00023	0.000077	3.02	0.003	0.055	1.18	—	—	—	—	—	—	—	—	—	—	—	—

negative effect on the R_s for 2012, 2013, and 2014, respectively.

3.4. Diurnal pattern of R_s

We chose the data from three consecutive sunny days in August of each year and analyzed the diurnal variations in the R_s. The hourly measurements revealed the cosine-like diurnal patterns of the R_s in the three ecosystems (Fig. 6). In the fen and meadow, the peak R_s was observed at approximately 1300 h, and the minimum value was observed between 0500 and 0700 h (Fig. 6a and b). However, variation in the R_s changed distinctly in the wet meadow, where two emission peaks were observed (Fig. 6c). The peak R_s occurred at noon (at approximately 1300 h) and early evening (1900 h), with the minimum occurring in the morning (at approximately 0800 h).

We plotted the R_s against the air temperature and two soil temperatures at depths of 5 cm and 10 cm. Hysteresis loops were produced in the relation between the R_s and the temperatures, which varied among the ecosystems (Supplementary Figs. S2, S3 and S4). In the fen and meadow, the R_s correlated most strongly with the air temperature due to the high R^2. In the wet meadow, however, diurnal variations in R_s were most closely related to variations in the soil temperature at a depth of 5 cm (Supplementary Table S4). After the effects of temperature had been removed, the residuals were generally positively correlated with PAR in the fen and wet meadow in 2012 (Fig. 7a), 2013 (Fig. 7b) and 2014 (Fig. 7c) but not in the meadow, indicating that photosynthesis is one of the main contributions to this diurnal hysteresis in wetland ecosystems (fen and wet meadow).

3.5. Temperature dependence of R_s among the ecosystems

The sensitivity of the R_s to temperature (Q_{10}) varied significantly among the three ecosystems except for the Q_{10} estimated from the soil temperature in 2013 (Fig. 8). The Q_{10} values related to the air temperatures in the wet meadow were significantly higher than those in the fen and meadow (Fig. 8a), whereas those related to the soil temperature showed marginal or no significant difference with the Q_{10} in the meadow (Fig. 8b). This result indicated that the sensitivity of the R_s to temperature would probably increase if the wetland dried from the fen to wet meadow and then decline as the wet meadow dried to the meadow. Since air temperature usually experiences larger fluctuations than the soil temperature, the Q_{10} estimated from the air temperature was lower than that from the soil temperature (fen: 1.47–1.48 vs. 1.78–2.29; wet meadow: 2.08–2.47 vs. 2.61–3.08; meadow: 1.41–1.58 vs. 2.24–2.77).

4. Discussion

4.1. R_s along the hydrological gradients

The annual carbon releases varied substantially from 129–193 g C m^{-2}yr^{-1} in the fen to 663–709 g C m^{-2}yr^{-1} in the meadow along the hydrological gradients. The annual respiration observed in the fen was within the wide range summarized by Raich and Schlesinger (1992) in northern bogs and mires (7–180 g C m^{-2}yr^{-1}) and that observed in boreal mires in Finland (79–347 g C m^{-2}yr^{-1}; Silvola et al., 1996). The annual R_s in the meadow was comparable to those measured during the similar period (2009–2012) at the same site (694–721 g C m^{-2}yr^{-1}; Wang et al., 2014) but was higher than had been previously measured from 1998 to 1999 (556 g C m^{-2}yr^{-1}; Cao et al., 2004). This difference was probably attributable to the progressive climate warming and soil drying in this area (Liu et al., 2018), which could promote CO_2 emissions from the soils. The R_s values observed in the wet meadow and meadow were approximately 1.1–3.0-fold and 2.3–6.6-fold higher than those reported for the heath and meadow in Arctic regions (103–292 g C m^{-2}yr^{-1}; Elberling, 2007; Morgner et al., 2010; Strebel et al., 2010); the reason may lie in the warmer and dryer conditions in the plateau
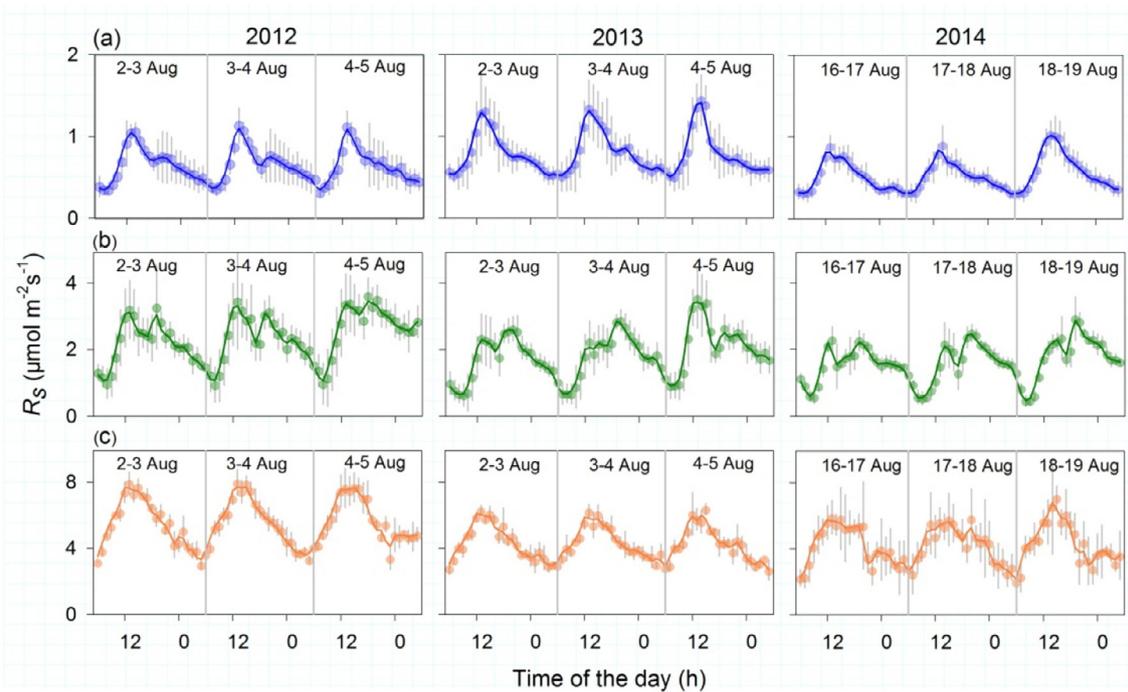
Fig. 6. Diurnal variations in soil respiration (R_s) on three consecutive sunny days for the thawed seasons of 2012, 2013 and 2014: (a) R_s for the fen; (b) R_s for the wet meadow; and (c) R_s for the meadow. The error bars represent the standard deviation of the means ($n = 5$ for the fen and wet meadow, and $n = 3$ for the meadow). The line is a 2-day running mean applied to the hourly data (2 column).

that accelerate soil carbon decomposition following permafrost degradation (Mu et al., 2017). Previous work from the Colorado Rocky Mountains, USA, reported the mean growing-season R_s across a broad soil moisture gradient (0.76–4.40 g C m^{-2}day^{-1}; Knowles et al., 2015; 2016), which were comparable to our results during growing seasons (0.57–3.0 g C m^{-2}day^{-1}). This similarity may help us define the range of growing-season R_s variation due to soil water availability in the alpine areas of the world.

For the three ecosystems, the increasing order of the R_s is the fen < wet meadow < meadow. The differences in the R_s among the three ecosystems could be due to their soil water conditions. In the Tibetan Plateau, wetland drying is expected due to permafrost thaw by rapid climate warming (Cheng and Wu, 2007), which is predicted to shift the fen to meadow during the hydrarch succession. Wetland drying from the fen to meadow could enhance soil CO_2 emissions in the future, as we observed here, but this pattern probably would not hold if the meadow soils became drier due to moisture limitation (Knowles et al., 2015). The increase in soil CO_2 emissions following wetland drying highlights the importance of considering changes in soil hydrological conditions to more accurately assess the carbon cycle response to permafrost thaw in alpine regions (Lawrence et al., 2015). In addition, other factors may also contribute to among-ecosystem R_s variations. For example, belowground biomass and soil carbon content could be positively associated with spatial variations in R_s (Geng et al., 2012; Wang et al., 2006). In this study, however, the belowground biomass and soil C content of the fen and wet meadow were significantly larger than those of the meadow ($P < 0.001$), but their annual R_s were much lower, indicating little effect of the belowground biomass and soil C on R_s along the hydrological gradients.

4.2. Seasonal dynamics of R_s and its abiotic controls

It is commonly accepted that R_s depends on air or soil temperature when water is not limiting (Bond-Lamberty and Thomson, 2010; Fang and Moncrieff, 2001; Lloyd and Taylor, 1994). In the current study, temperature was the dominant factor influencing seasonal

variation in the R_s in the thawed season. Notably, the air temperature exerted a larger control than soil on CO_2 variation in the fen and wet meadow. Chimner (2004) also found that R_s was more correlated to air temperature than to soil temperature in a suite of tropical peatlands. This finding may be explained by the different soil layers of CO_2 production among the ecosystems. Water is generally in excess in wetlands, so it is probable that soil CO_2 production concentrates on the soil surface, which has more access to oxygen and is more influenced by air temperature fluctuations.

The R_s generally decreased with an increasing water table in the fen or soil moisture in the wet meadow, suggesting that water is often in excess in these sites, limiting the diffusivity of O_2 in the soil and thus impeding decomposition and CO_2 production (Linn and Doran, 1984). Several controlled experiments with manipulative increasing of the water table also observed a similar pattern (Chimner and Cooper, 2003; Yang et al., 2013). However, CH_4 emissions, another greenhouse gas, would increase with the water table in this wetland (Song et al., 2015), implying that the CO_2 reduction induced by the water table increase could be offset to some extent by stimulated CH_4 emissions. In the meadow, soil moisture had a positive (2012), little (2013) and a negative (2014) impact on the R_s. The different effects of soil moisture on the R_s were most likely related to variations in rainfall among the three years. Soil water was depleted in the dry year of 2012 (367 mm), moderate in the year of 2013 (403 mm), and excessive in the wet year of 2014 (573 mm). Soil water in 2012 and 2014 could lead to water limitation and oxygen or diffusion limitation, respectively, and then constrain microbial activities in the decomposition processes. Therefore, soil moisture would have the opposite impact on R_s in 2012 and 2014.

4.3. CO_2 bursts in the spring thawing season

A notable feature in the seasonal variation in R_s was the bursts of CO_2 during the thawing season in the wetland, especially in the fen, which led to a large contribution of cumulative R_s to annual respiration (20–38% for the fen and 13–17% for the wet meadow) during this
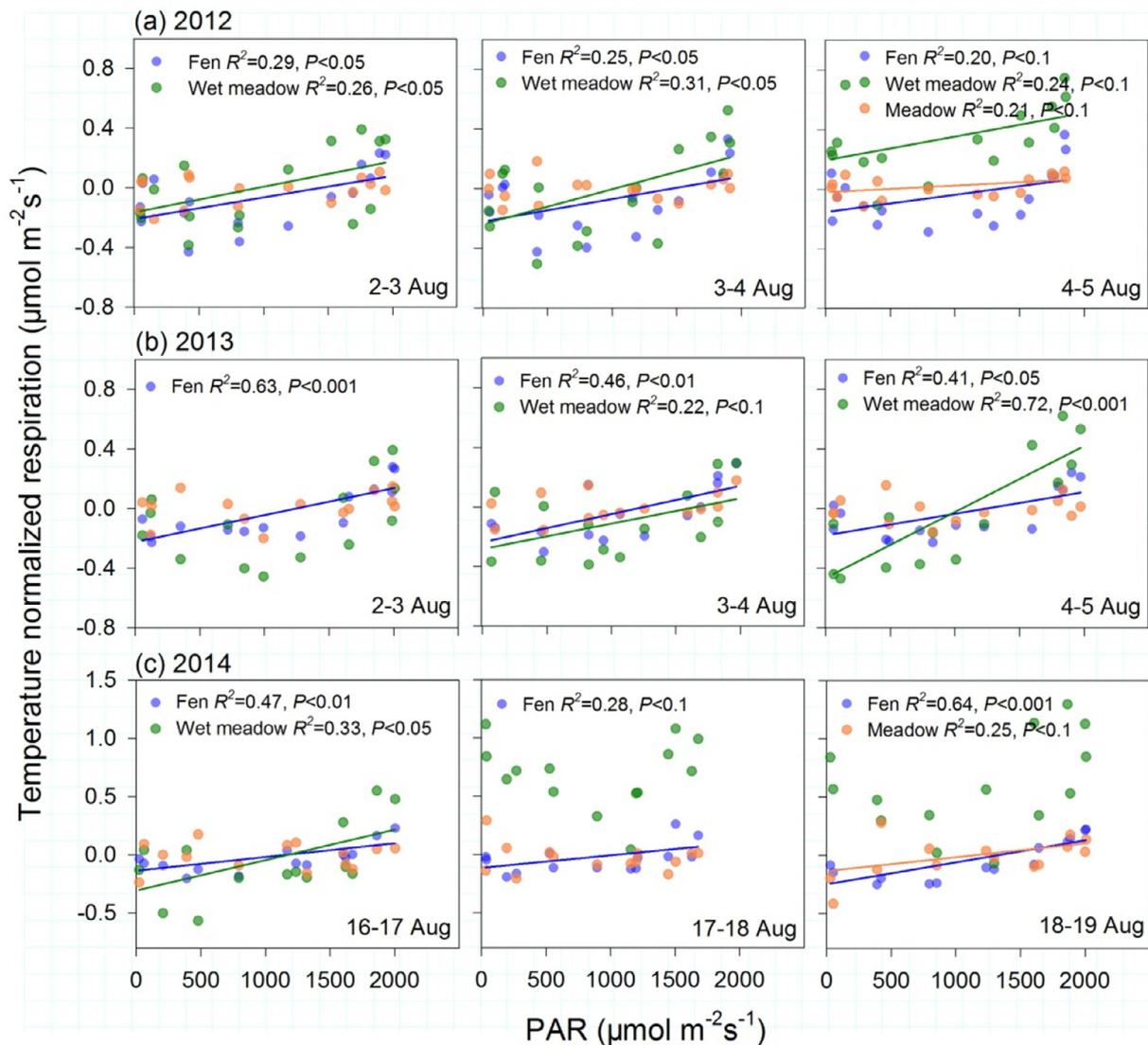
Fig. 7. The relation between temperature-normalized respiration and photosynthetically active radiation (PAR) during the daytime (PAR > 0) on three consecutive sunny days for the soil-thawed seasons of 2012 (a), 2013 (b) and 2014 (c). Temperature-normalized respiration is calculated as the differences of the observed and fitted hourly mean soil respiration from the temperature model. The model is indicated by Eq. (2). The variable of air or soil temperatures with the largest explanatory power was included in the model according to Table S4 (1.5 column).

period. This contribution suggests that in the nongrowing season (including the thawing season), R_s plays an important role in the carbon cycle and can never be ignored (Fahnestock et al., 1999). A burst of CO_2 from the soil has also been observed relative to soil thawing in tundra (Elberling and Brandt, 2003; Nordstroem et al., 2001) and forest ecosystems (Goldberg et al., 2008). In winter, a large portion of the produced CO_2 cannot be released into the atmosphere due to the isolation of the ice and frozen soil surface (Oechel et al., 1997). When the frozen surface is thawing in the following spring, the release of trapped CO_2 is expected to occur, leading to the emission burst. However, the CO_2 burst exhibited large spatial heterogeneity along the hydrological gradient, with little CO_2 increase during thawing in the meadow. We speculated that the soil water conditions regulated the biophysical effect of spring thawing on the soil CO_2 emission, which increased with soil water content. The lack of CO_2 bursts in the meadow may have been caused by little CO_2 being trapped beneath the soil due to the relatively low soil moisture. Similarly, Elberling and Brandt (2003) found that the trapping of CO_2 in frozen soil during the winter was positively correlated with the soil moisture.

4.4. Diurnal variation in R_s

Although diurnal hysteresis for R_s was observed, along with a rise in temperature, the relationship was more linear and the hysteresis effect was less pronounced for R_s plotted with air temperature than that with soil temperatures in the fen and meadow and for R_s plotted with soil temperature at 5 cm than that with other temperatures in the wet meadow. Since the temperature-independent component of the diurnal variation could be generally explained by variation in PAR in the fen and wet meadow at day time, we postulate that the diurnal variation in R_s may also be regulated by photosynthesis, as documented in previous studies (e.g., Liu et al., 2006; Tang et al., 2005). The dependence of soil respiration on photosynthesis may be because of the source of carbohydrate for autotrophic R_s and possibly also for heterotrophic R_s through root exudates provided by the recent photosynthate. However, photosynthesis may not drive soil respiration in the meadow due to the lack of relation between the temperature-independent R_s and the PAR. The possible reason for the small effect of photosynthesis could be that the relatively low soil moisture in the meadow reduced the diffusion of photoassimilated carbon through the soil and resulted in limitations in
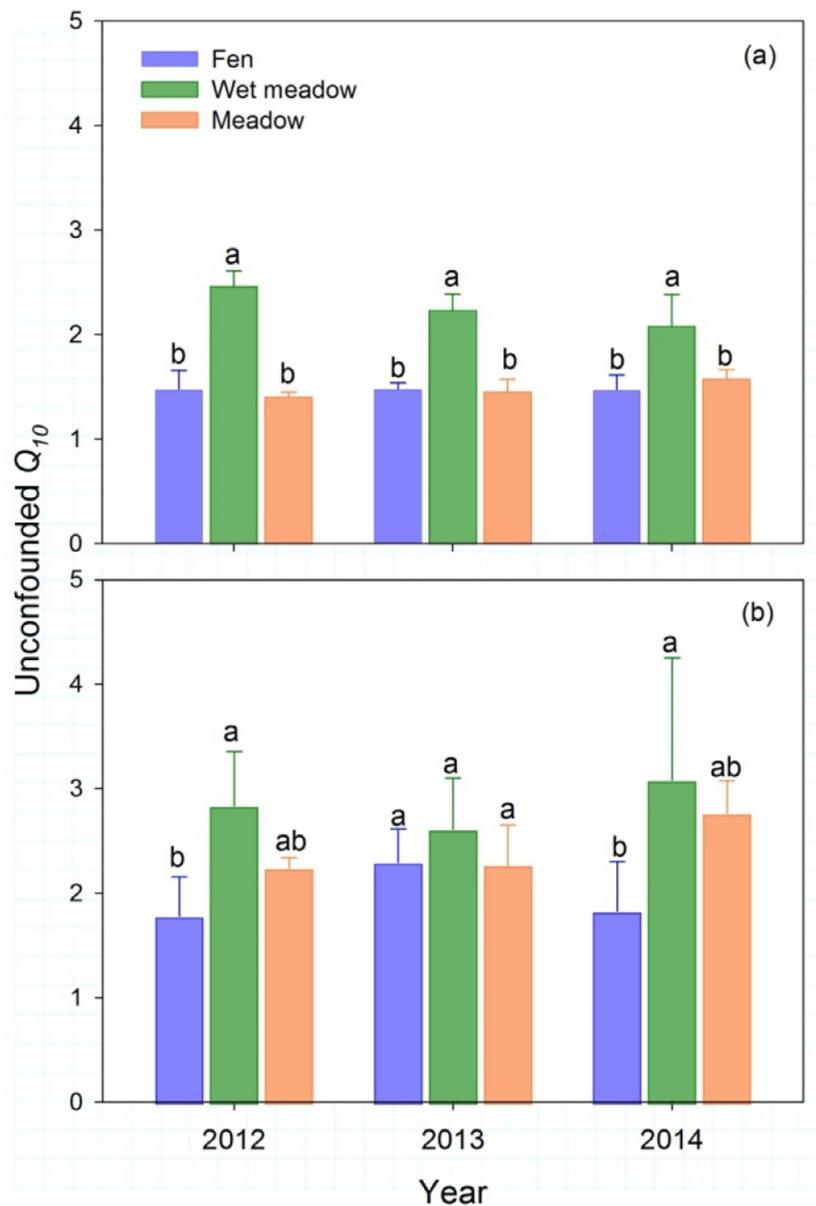
Fig. 8. The temperature sensitivity of soil respiration (unconfounded Q_{10}) for the fen, wet meadow and meadow during the thawed seasons of 2012, 2013 and 2014. Q_{10} was estimated from (a) air temperature and (b) soil temperature at a 5-cm depth. The error bars represent standard deviations of the means ($n = 5$ for the fen and wet meadow, and $n = 3$ for the meadow). Different letters in the same year represent significant differences in Q_{10} among the three ecosystems ($P < 0.05$) (single column).

the substrate supply for microbial respiration (Davidson et al., 2006). This phenomenon suggests that other factors, rather than photosynthesis, are driving the diurnal variation in R_s in addition to soil temperature in the meadow. If the lag between R_s and temperature was controlled solely by the physical processes through the soil, the R_s would be expected to lag behind the temperature because the gas transfer through the soil would take time. However, such a hypothesis is not supported by our observations, which showed peak R_s occurred before the peak air or soil temperature, indicating that soil physical processes (e.g., gas transfer) alone caused very little hysteresis. Overall, the results highlight the variable effect of photosynthesis on regulating the diurnal variation in R_s along the hydrological gradients.

In the current study, a specific diurnal pattern of R_s with two obvious peaks was observed in the wet meadow. The first emission peak occurred at noon (1300 h), which coincided with the time of peak PAR, suggesting that the first peak may be related to photosynthesis at this time. The R_s can lag shortly behind PAR for low grasses and herbs (e.g.,

minimum 1-h lag reported by Kuzyakov and Gavrichkova (2010)), which could explain the occurrence of the first R_s peak at approximately the time of the maximum PAR. The second peak of R_s in early evening (1900 h) could be associated with the temperature peaking at approximately 1500–1600 h for the air and 1800 h for the soil. The lag between the peak CO_2 emission and peak temperature may result from the physical processes in the soil.

4.5. Temperature sensitivity of R_s along the hydrological gradients

The unconfounded Q_{10} in the fen and meadow estimated from the air temperature was similar (mean Q_{10} of 1.5) and was very close to the global scale sensitivity of soil respiration ($Q_{10} = 1.5$; Bond-Lamberty and Thomson, 2010) and ecosystem respiration ($Q_{10} = 1.4$; Mahecha et al., 2010) to air temperature. With reference to soil temperature, the mean Q_{10} values for the three ecosystems ranged from 2.0 to 2.8 and were higher than those estimated after minimizing the

seasonality of vegetation activity in the Northern Hemisphere ($Q_{10} = 1.5$; Wang et al., 2010) and higher than the global scale optimal temperature sensitivity of soil respiration estimated from inverse modeling methods ($Q_{10} = 1.4$–2.0; Ise and Moorcroft, 2006; Zhou et al., 2015).

Wang et al. (2018) reported the convergence in the Q_{10} (mean = 2.4) estimated from soil temperature for the mesic grassland and meadow in the Tibetan Plateau. Similarly, the estimated Q_{10} values for the wet meadow in the current study showed marginally higher or no significant difference with those for the meadow but were significantly higher than those for the fen, implying that the temperature sensitivity of the R_s increases with the wetland drying from fen to wet meadow and then tends to decline from the wet meadow to meadow. A possible explanation for the observed Q_{10} variation among the ecosystems is the hydrological difference along the slope. As reviewed in Davidson and Janssens (2006), both flooding and drought could constrain the temperature sensitivities of decomposition. Flooding, as a condition of the fen, slows oxygen diffusion to decomposition reaction sites and impedes aerobic decomposition and CO_2 production (Sahrawat, 2004). Drought, as it occurs in the meadow, could limit the diffusion of extracellular enzymes and soluble substrates due to the thin soil water films and reduce the substrate availability at the reaction microsites. In these cases, the CO_2 emission would be less responsive to temperature in the fen or meadow than in the wet meadow with intermediate moisture content.

Another possible explanation for the variation in temperature dependency of R_s among the ecosystems is the differences in microbial community composition. Li et al. (2017) reported that the community structure of bacteria, archaea and eukaryotes exhibited differences along the hydrological gradients at the same study site. The shift in the microbial community structure could alter the temperature sensitivity of the respiration through changes in the enzyme substrate affinities and the various abilities of different groups of microbes to grow within the observed temperature regimes (Bradford et al., 2008; Mäkiranta et al., 2009). However, this proposed mechanism was merely speculative, and more research is needed to confirm the shift of the microbial community as a mechanism responsible for the change in temperature sensitivity along the hydrological gradients.

5. Conclusions

This study showed the large contribution of the spring thawing effect on the annual soil CO_2 emission due to the CO_2 burst in the wetland ecosystems, especially in the fen (20–38%), indicating that R_s during the thawing season plays an important role in the carbon cycles in alpine wetland ecosystems. Thus, the spring thawing effect should be incorporated into the Earth system models for more accurate estimation of carbon budgets in alpine wetlands and an assessment of the carbon-climate feedbacks. Our results also suggest that wetland dryness will trigger large carbon loss from the soils. Although predicted wetland drying from the fen to wet meadow could enhance the temperature sensitivity of soil CO_2 emission, that is, the CO_2 emission would be accelerated in response to climate warming in the future, further drying from the wet meadow to meadow could probably decrease the response. These results could help us to better understand how ecosystem processes respond to long-term climate dynamics, not only on the Tibetan Plateau but also in boreal, arctic and alpine ecosystems worldwide.

Declaration of Competing Interest

The authors declare that they have no known competing financial interests or personal relationships that could have appeared to influence the work reported in this paper.

Acknowledgements

Supplementary materials

Supplementary material associated with this article can be found, in the online version, at doi:10.1016/j.agrformet.2019.107854.

References

Aselmann, I., Crutzen, P.J., 1989. Global distribution of natural freshwater wetlands and rice paddies, their net primary productivity, seasonality and possible methane emissions. J. Atmos. Chem. 8 (4), 307–358.

Baumann, F., He, J.-.S., Schmidt, K., Kühn, P., Scholten, T., 2009. Pedogenesis, permafrost, and soil moisture as controlling factors for soil nitrogen and carbon contents across the Tibetan Plateau. Global Change Biol. 15 (12), 3001–3017.

Bond-Lamberty, B., Thomson, A., 2010. Temperature-associated increases in the global soil respiration record. Nature 464 (7288), 579–582.

Bradford, M.A., et al., 2008. Thermal adaptation of soil microbial respiration to elevated temperature. Ecol. Lett. 11 (12), 1316–1327.

Cao, G., Tang, Y., Mo, W., Wang, Y., Li, Y., Zhao, X., 2004. Grazing intensity alters soil respiration in an alpine meadow on the Tibetan plateau. Soil Biol. Biochem. 36, 237–243.

Cheng, G., Wu, T., 2007. Responses of permafrost to climate change and their environmental significance, Qinghai-Tibet Plateau. J. Geophys. Res. 112 (F02S03).

Chimner, R.A., 2004. Soil respiration rates of tropical peatlands in Micronesia and Hawaii. Wetlands 24 (1), 51–56.

Chimner, R.A., Cooper, D.J., 2003. Influence of water table levels on CO_2 emissions in a Colorado subalpine fen: an in situ microcosm study. Soil Biol. Biochem. 35, 345–351.

Davidson, E.A., Belk, E., Boone, R.D., 1998. Soil water content and temperature as independent or confounded factors controlling soil respiration in a temperate mixed hardwood forest. Global Change Biol. 4 (2), 217–227.

Davidson, E.A., Janssens, I.A., 2006. Temperature sensitivity of soil carbon decomposition and feedbacks to climate change. Nature 440 (7081), 165–173.

Davidson, E.A., Janssens, I.A., Luo, Y., 2006. On the variability of respiration in terrestrial ecosystems: moving beyond Q_{10}. Global Change Biol. 12 (2), 154–164.

Elberling, B., 2007. Annual soil CO_2 effluxes in the high Arctic: the role of snow thickness and vegetation type. Soil Biol. Biochem. 39, 646–654.

Elberling, B., Brandt, K.K., 2003. Uncoupling of microbial CO_2 production and release in frozen soil and its implications for field studies of arctic C cycling. Soil Biol. Biochem. 35 (2), 263–272.

Fahnestock, J.T., Jones, M.H., Welker, J.M., 1999. Wintertime CO_2 efflux from Arctic soils: implications for annual carbon budgets. Global Biogeochem. Cycles 13 (13), 775–780.

Fang, C., Moncrieff, J.B., 2001. The dependence of soil CO_2 efflux on temperature. Soil Biol. Biochem. 33, 155–165.

Gaumont-Guay, D., et al., 2006. Interpreting the dependence of soil respiration on soil temperature and water content in a boreal aspen stand. Agric. For. Meteorol. 140 (1), 220–235.

Geng, Y., et al., 2012. Soil respiration in tibetan alpine grasslands: belowground biomass and soil moisture, but not soil temperature, best explain the large-scale patterns. PLoS ONE 7 (4), e34968.

Goldberg, S.D., Muhr, J., Borken, W., Gebauer, G., 2008. Fluxes of climate-relevant trace gases between a Norway spruce forest soil and atmosphere during repeated freeze–thaw cycles in mesocosms. J. Plant Nutr. Soil Sci. 171 (5), 729–739.

Gorham, E., 1995. Biotic Feedbacks in the Global Climatic System. Oxford University Press, New York.

Groffman, P., Hardy, J., Driscoll, C., Fahey, T., 2006. Snow depth, soil freezing, and fluxes of carbon dioxide, nitrous oxide and methane in a northern hardwood forest. Global Change Biol. 12 (9), 1748–1760.

Gu, L., Hanson, P.J., Post, W.M., Liu, Q., 2008. A novel approach for identifying the true temperature sensitivity from soil respiration measurements. Global Biogeochem. Cycles 22, GB4009.

Henry, H.A.L., 2007. Soil freeze–thaw cycle experiments: trends, methodological weaknesses and suggested improvements. Soil Biol. Biochem. 39 (5), 977–986.

IPCC, 2013. Climate change 2013: the physical science basis. In: Working Group I Contribution to the Fifth Assessment Report of the Intergovernmental Panel on Climate Change. New York. Cambridge University Press, New York.

Ise, T., Moorcroft, P.R., 2006. The global-scale temperature and moisture dependencies of soil organic carbon decomposition: an analysis using a mechanistic decomposition model. Biogeochemistry 80 (3), 217–231.

Kim, D.-.G., Vargas, R., Bond-Lamberty, B., Turetsky, M.R., 2012. Effects of soil rewetting and thawing on soil gas fluxes: a review of current literature and suggestions for future research. Biogeosciences 9, 2459–2483.

Knapp, A.K., et al., 2008. Consequences of more extreme precipitation regimes for terrestrial ecosystems. Bioscience 58 (9), 811–821.

Knowles, J.F., Blanken, P.D., Williams, M.W., 2015. Soil respiration variability across a soil moisture and vegetation community gradient within a snow-scoured alpine meadow. Biogeochemistry 125, 185–202.

Knowles, J.F., Blanken, P.D., Williams, M.W., 2016. Wet meadow ecosystems contribute

the majority of overwinter soil respiration from snow-scoured alpine tundra. J. Geophys. Res. 121, 1118–1130.

Kuzyakov, Y., Gavrichkova, O., 2010. Time lag between photosynthesis and carbon dioxide efflux from soil: a review of mechanisms and controls. Global Change Biol. 16 (12), 3386–3406.

Lawrence, D.M., Koven, C.D., Swenson, S.C., Riley, W.J., Slater, A.G., 2015. Permafrost thaw and resulting soil moisture changes regulate projected high-latitude CO_2 and CH_4 emissions. Environ. Res. Lett. 10, 094011.

Li, Y., et al., 2017. Distinct soil microbial communities in habitats of differing soil water balance on the Tibetan Plateau. Sci. Rep. 7, 46407.

Liang, N., Teramoto, M., Takagi, M., Zeng, J., 2017. High-resolution data on the impact of warming on soil CO_2 efflux from an Asian monsoon forest. Sci. Data 4, 170026.

Linn, D.M., Doran, J.W., 1984. Effect of water-filled pore space on carbon dioxide and nitrous oxide production in tilled and nontilled soils. Soil Sci. Soc. Am. J. 48 (6), 1267–1272.

Liu, H., et al., 2018. Shifting plant species composition in response to climate change stabilizes grassland primary production. Proc. Natl. Acad. Sci. U.S.A. 115, 4051–4056.

Liu, Q., et al., 2006. Temperature-independent diel variation in soil respiration observed from a temperate deciduous forest. Global Change Biol. 12 (11), 2136–2145.

Liu, X., Chen, B., 2000. Climatic warming in the Tibetan Plateau during recent decades. Int. J. Climatol. 20 (14), 1729–1742.

Liu, X.D., Cheng, Z.G., Zhang, R., 2009. The A1B scenario projection for climate change over the Tibetan Plateau in the next 30-50 years. Plateau Meteorol. 28 (3), 475–484.

Lloyd, J., Taylor, J.A., 1994. On the temperature dependence of soil respiration. Funct. Ecol. 8 (3), 315–323.

Mäkiranta, P., et al., 2009. Indirect regulation of heterotrophic peat soil respiration by water level via microbial community structure and temperature sensitivity. Soil Biol. Biochem. 41 (4), 695–703.

Ma, Q., et al., 2017. Aboveground and belowground biomass relationships in the Zoige peatland, eastern Qinghai–Tibetan Plateau. Wetlands 1–9.

Mahecha, M.D., et al., 2010. Global convergence in the temperature sensitivity of respiration at ecosystem level. Science 329 (5993), 838–840.

Matthews, E., Fung, I., 1987. Methane emission from natural wetlands: global distribution, area, and environmental characteristics of sources. Global Biogeochem. Cycles 1 (1), 61–86.

Matzner, E., Borken, W., 2008. Do freeze-thaw events enhance C and N losses from soils of different ecosystems? A review. Eur. J. Soil Sci. 59 (2), 274–284.

Miao, G.F., et al., 2013. The effect of water table fluctuation on soil respiration in a lower coastal plain forested wetland in the southeastern us. J. Geophys. Res. 118 (4), 1748–1762.

Morgner, E., Elberling, B., Strebel, D., Cooper, E.J., 2010. The importance of winter in annual ecosystem respiration in the high Arctic: effects of snow depth in two vegetation types. Polar Res 29, 58–74.

Mu, C.C., Abbott, B.W., Zhao, Q., Su, H., Wang, S.F., Wu, Q.B., Zhang, T.J., Wu, X.D., 2017. Permafrost collapse shifts alpine tundra to a carbon source but reduces N_2O and CH_4 release on the northern Qinghai-Tibetan Plateau. Geophys. Res. Lett. 44, 8945–8952.

Muhr, J., Borken, W., Matzner, E., 2009. Effects of soil frost on soil respiration and its radiocarbon signature in a Norway spruce forest soil. Global Change Biol. 15, 782–793.

Niu, Z., Zhang, H., Wang, X., Yao, W., Zhou, D., Zhao, K., Zhao, H., Li, N., Huang, H., Li, C., Yang, J., Liu, C., Liu, S., Wang, L., Li, Z., Yang, Z., Qiao, F., Zheng, Y., Chen, Y., Sheng, Y., Gao, X., Zhu, W., Wang, W., Wang, H., Weng, Y., Zhuang, D., Liu, J., Luo, Z., Cheng, X., Guo, Z., Gong, P., 2012. Mapping wetland changes in China between 1978 and 2008. Chin. Sci. Bull. 57, 2813–2823.

Nordstroem, C., Soegaard, H., Christensen, T.R., Friborg, T., Hansen, B.U., 2001. Seasonal carbon dioxide balance and respiration of a high-arctic fen ecosystem in NE-Greenland. Theor. Appl. Climatol. 70 (1), 149–166.

Oechel, W.C., Vourlitis, G., Hastings, S.J., 1997. Cold season CO_2 emission from arctic soils. Global Biogeochem. Cycles 11, 163–172.

Papale, D., Valentini, R., 2003. A new assessment of European forests carbon exchanges by eddy fluxes and artificial neural network spatialization. Global Change Biol. 9 (4), 525–535.

Phillips, C.L., Nickerson, N., Risk, D., Bond, B.J., 2011. Interpreting diel hysteresis between soil respiration and temperature. Global Change Biol. 17 (1), 515–527.

Raich, J.W., Schlesinger, W.H., 1992. The global carbon dioxide flux in soil respiration and its relationship to vegetation and climate. Tellus B 44, 81–99.

Ran, Y., Li, X., Cheng, G., Zhang, T., Wu, Q., Jin, H., Jin, R., 2012. Distribution of permafrost in China: an overview of existing permafrost maps. Permafr. Perigl. Proc. 23, 322–333.

Reichstein, M., et al., 2002. Ecosystem respiration in two Mediterranean evergreen Holm Oak forests: drought effects and decomposition dynamics. Funct. Ecol. 16 (1), 27–39.

Riveros-Iregui, D.A., et al., 2007. Diurnal hysteresis between soil CO_2 and soil temperature is controlled by soil water content. Geophys. Res. Lett. 34, L17404.

Ryan, M.G., Law, B.E., 2005. Interpreting, measuring, and modeling soil respiration. Biogeochemistry 73 (1), 3–27.

Sahrawat, K.L., 2004. Organic matter accumulation in submerged soils. Adv. Agron. 81 (03), 169–201.

Savage, K.E., Davidson, E.A., 2001. Interannual variation of soil respiration in two New England forests. Global Biogeochem. Cycles 15 (2), 337–350.

Schimel, J., Balser, T.C., Wallenstein, M., 2007. Microbial stress-response physiology and its implications for ecosystem function. Ecology 88 (6), 1386–1394.

Schuur, E.A.G., et al., 2015. Climate change and the permafrost carbon feedback. Nature 520, 171–179.

Silvola, J., Alm, J., Ahlholm, U., Nykanen, H., Martikainen, P.J., 1996. CO_2 fluxes from peat in boreal mires under varying temperature and moisture conditions. J. Ecol. 84, 219–228.

Strebel, D., Elberling, B., Morgner, E., Knicker, H.E., Cooper, E., 2010. Cold-season soil respiration in response to grazing and warming in High-Arctic Svalbard. Polar Res 29, 46–57.

Song, W., Wang, H., Wang, G., Chen, L., Jin, Z., Zhuang, Q., He, J.-.S., 2015. Methane emissions from an alpine wetland on the Tibetan Plateau: neglected but vital contribution of the nongrowing season. J. Geophys. Res. 120. https://doi.org/10.1002/2015JG003043.

Sun, H.L., Zheng, D., 1996. Formation and Evolution of Qinghai-Xizang Plateau. Shanghai Science and Technology Press, Shanghai.

Tang, J., Baldocchi, D.D., Xu, L., 2005. Tree photosynthesis modulates soil respiration on a diurnal time scale. Global Change Biol. 11 (8), 1298–1304.

Wang, C., Yang, J., Zhang, Q., 2006. Soil respiration in six temperate forests in China. Global Change Biol. 12 (11), 2103–2114.

Wang, S., Sheng, Y., Wu, J., Li, J., Chen, J., 2015. The characteristics and changing tendency of permafrost in the source of the Datong River, Qilian Mountains. J. Glaciol. Geocryol 37 (1), 27–37.

Wang, X., et al., 2010. Are ecological gradients in seasonal Q10 of soil respiration explained by climate or by vegetation seasonality? Soil Biol. Biochem 42 (10), 1728–1734.

Wang, Y., et al., 2014. Non-growing-season soil respiration is controlled by freezing and thawing processes in the summer monsoon-dominated Tibetan alpine grassland. Global Biogeochem. Cycles 28. https://doi.org/10.1002/2013GB004760.

Wang, Y., et al., 2018. Convergence in temperature sensitivity of soil respiration: evidence from the Tibetan alpine grasslands. Soil Biol. Biochem. 122, 50–59.

Yang, J., et al., 2013. Effect of water table level on CO_2, CH_4 and N_2O emissions in a freshwater marsh of Northeast China. Soil Biol. Biochem. 61 (6), 52–60.

Yang, Y., Fang, J., Ji, C., Han, W., 2009. Above- and belowground biomass allocation in Tibetan grasslands. J. Veg. Sci. 20 (1), 177–184.

Yu, L., et al., 2013. A comparison of methane emission measurements using eddy covariance and manual and automated chamber-based techniques in Tibetan Plateau alpine wetland. Environ. Pollut. 181, 81–90.

Yuste, J., Janssens, I., Carrara, A., Ceulemans, R., 2004. Annual Q10 of soil respiration reflects plant phenological patterns as well as temperature sensitivity. Global Change Biol 10 (2), 161–169.

Zhang, Y., Wang, G., Wang, Y., 2011. Changes in alpine wetland ecosystems of the Qinghai-Tibetan plateau from 1967 to 2004. Environ. Monit. Assess 180, 189–199.

Zhou, T., Shi, P., Hui, D., Luo, Y., 2015. Global pattern of temperature sensitivity of soil heterotrophic respiration (Q10) and its implications for carbon-climate feedback. J. Geophys. Res. 114 (G2), 271–274.